Fluorescence spectrum, thermal properties, and continuous-wave laser performance of the mixed crystal Nd:$Lu_{0.99}La_{0.01}VO_4$

Yunzheng Wang (王云征)[1], Bin Zhao (赵 斌)[2], Zhuang Zhuo (卓 壮)[1*], Jingxuan Wang (王静轩)[1], Liqiang Zhang (张丽强)[1], Huabing Qin (秦华兵)[3], and Jianzhong Chen (陈建中)[2]

[1]*College of Information Science and Engineering, Shandong University, Jinan 250100, China*

[2]*College of Chemistry and Chemical Engineering, Fuzhou University, Fuzhou 350108, China*

[3]*Shandong Inspur Huaguang Optoelectronics Co., Ltd., Weifang, 261061, China*

[*]*Corresponding author: zhuozhuang@sdu.edu.cn*

Received September 25, 2013; accepted November 12, 2013; posted online December 9, 2013

The fluorescence spectrum and thermal properties of the mixed crystal Nd:$Lu_{0.99}La_{0.01}VO_4$ are determined. The strongest emission peak located at 1065.6 nm had a full width at half maximum (FWHM) of 2.1 nm. Continuous-wave (CW) laser performance is demonstrated by a compact planar–planar cavity that is end-pumped by a diode laser. The laser output characteristics are investigated by using output couplers with different transmissions. A maximum CW output power of 8.09 W was obtained at an incident pump power of 19.4 W, which corresponds to an optical-to-optical conversion efficiency of 41.7% and a slope efficiency of 54.6%. The dependence of optimum transmission on pump power is calculated theoretically and is found to be consistent with experimental results.

OCIS codes: 140.3380, 350.6830, 140.3480, 140.3580.

doi: 10.3788/COL201311.121404.

Presently, diode-pumped solid-state lasers have been widely used in numerous application fields, including material processing, medical devices, and scientific instruments. In such applications, laser crystals serve a key function in determining laser performance. Compared with Nd:YAG, Nd-doped single vanadate crystals, such as Nd:YVO_4[1–3], Nd:$GdVO_4$[4–6], and Nd:$LuVO_4$[7–9], have been proven to be excellent gain mediums for diode-pumped solid-state laser operations at modest output power levels because of their broad absorption bandwidth, large emission cross sections, and polarized emission. However, large emission cross sections and short upper-level lifetimes result in small energy storage capacities in the Q-switching operation regime. In addition, a narrow fluorescence width leads to difficulty in obtaining sub-picosecond pulses during mode-locking operation. The inhomogeneous broadening of the spectra enables Nd-doped mixed vanadate crystals to reduce emission cross sections and to increase fluorescence lifetime while retaining the advantages of single vanadate crystals. A large number of mixed vanadate crystals, such as Nd:$La_xGd_{1-x}VO_4$[10], Nd:$La_xY_{1-x}VO_4$[11,12], Nd:$Lu_xY_{1-x}VO_4$[13,14], Nd:Gd_x $Lu_{1-x}VO_4$[15], Nd:Y_x $Gd_{1-x}VO_4$[16], and Nd:$Gd_{0.33}Lu_{0.33}$ $Y_{0.33}VO_4$[17], have been grown and demonstrated to be excellent gain candidates in high peak power Q-switching and mode-locking laser operations. In 2012, Huang *et al.* reported on the continuous-wave (CW) and actively Q-switching laser performance of Nd:$Lu_{0.99}La_{0.01}VO_4$ at 1.06 μm; they obtained an output power of 6.26 W for CW operation and an average output power of 6.06 W for Q-switching operation[18].

In this letter, we report on the fluorescent spectral properties of the mixed crystal Nd:$Lu_{0.99}La_{0.01}VO_4$. We measured its thermal focal length based on incident pump power. The laser behavior of Nd:$Lu_{0.99}La_{0.01}VO_4$ was investigated sufficiently by using a compact planar–planar resonant cavity at different output couplers. A maximum CW output power of 8.09 W was obtained at an incident pump power of 19.4 W, which corresponds to an optical-to-optical conversion efficiency of 41.7% and a slope efficiency of 54.6%. Finally, optimum transmission was theoretically investigated at different pump powers. The results exhibit fair agreement with experimental data.

The mixed crystal Nd:$Lu_{0.99}La_{0.01}VO_4$, which is an isomorphism of Nd:$LuVO_4$, was grown via the Czochralski method with a Nd doping concentration of 0.25%. La ions replaced a fraction of Lu ions, and the crystal retained its tetragonal symmetry. The fluorescence spectrum was obtained by an Edinburgh FLS920 fluorescence spectrophotometer (Edinburgh Instruments Ltd., UK) at room temperature. Figure 1 shows the fluorescence spectrum ranging from 960 to 1450 nm with a resolution of 0.15 nm.

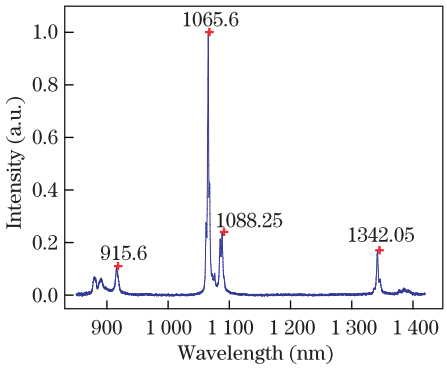

Fig. 1. Fluorescence spectrum of the mixed crystal Nd:$Lu_{0.99}La_{0.01}VO_4$.

Three main emission peaks were observed with central wavelengths located at 915.6, 1065.6, and 1342.05 nm, which are associated with the energy level transitions $^4F_{3/2} \rightarrow ^4I_{9/2}$, $^4F_{3/2} \rightarrow ^4I_{11/2}$, and $^4F_{3/2} \rightarrow ^4I_{13/2}$ of Nd^{3+},respectively. The strongest emission peak located at 1065.6 nm had a full-width at half-maximum (FWHM) of 2.1 nm. The introduction of La^{3+} expanded the fluorescence line width in Nd:$Lu_{0.99}La_{0.01}VO_4$ crystals compared with that in Nd:$LuVO_4$[14] because of the structural disorder induced inside the crystal[19].

In high-power solid-state lasers, the thermal effect serves a vital function in further increasing output power because of its significant effect on cavity stability, beam quality, and overlapping efficiency. Thus, the thermal focal length of the laser medium must be measured against pump power to optimize high-power solid-state lasers. The thermal focal length was determined based on stability theory of resonators[20]. Figure 2 shows a schematic of the setup used to measure the thermal focal length of Nd:$Lu_{0.99}La_{0.01}VO_4$ crystal.

The crystal was cut along the a axis with the dimensions 3×3×5 (mm) ($a \times c \times a$). The end faces were polished and antireflection (AR) coating was applied at 808 and 1064 nm. To remove heat and prevent thermally induced fracture, the mixed crystal was wrapped with a piece of thin In foil and inserted into a slot in a water-cooled Cu block at a temperature of 20 °C. The mixed crystal Nd:$Lu_{0.99}La_{0.01}VO_4$ was pumped by a fiber-coupled diode laser at 808 nm (LIMO Lissotschenko Mikrooptik, GmbH, Germany). The fiber core was 400 μm and had a numerical aperture of 0.22. The pump beam was coupled into the laser crystal via relay optics to produce a beam diameter of approximately 480 μm inside the crystal. The rear mirror M1 was AR coated at 808 nm and high-reflection coating was applied at 1064 nm. The output coupler M2 had a transmission of 11% at 1064 nm. M1 and M2 were both plane mirrors, and the crystal was placed near M1. The thermal focal length at various pump powers was determined according to cavity stability theory, as shown in Fig. 3. The dots represented the experimental data on the thermal focal length, whereas the red solid line was the fitted curve, which was achieved for the following optimization by the inverse proportional function[21]:

$$f_t = \frac{517.45}{P_{in} - 6.64} + 21.96, \quad (1)$$

where f_t is the thermal focal length and P_{in} is the incident pump power.

The CW laser operation of Nd:$Lu_{0.99}La_{0.01}VO_4$ was realized through a planar-planar resonant cavity end-pumped by a diode laser. The experimental setup

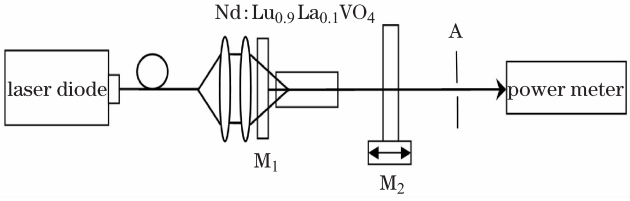

Fig. 2. Schematic of the experimental setup used to measure the thermal focal length.

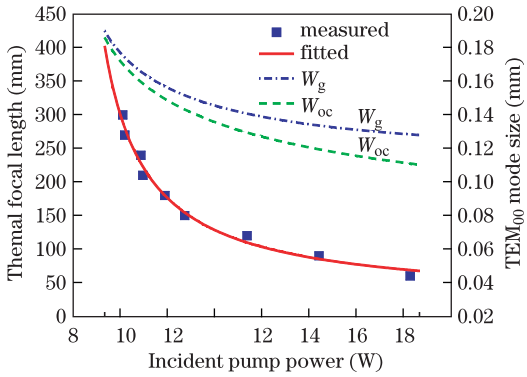

Fig. 3. (Color online) Thermal focal length and TEM_{00} mode size. The dot and the red solid line respectively denote the experimental data and the fitted curve of the thermal focal length versus the pump power. The upper two lines are the TEM_{00} mode sizes on the crystal w_g (dot-dashed) and the output coupler w_{oc} (dashed), respectively.

was similar to that shown in Fig. 2. The cavity length was fixed at 30 mm, and the output coupler M2 had four different transmissions, i.e., 7%, 11%, 20%, and 30%. The laser spectrum was recorded by an Anritsu MS9710C optical spectrum analyzer (Anritsu Company, USA). The output power was measured by using an LP-3C power meter (Institute of Physics, Chinese Academy of Sciences, China). The laser was experimentally optimized to generate a fundamental laser mode and to achieve the highest optical conversion efficiency at different transmissions of the output couplers. Figure 4 shows the change in output power versus the incident pump power at different output couplers, in which the dots represent the experimental data, and the solid lines denote the theoretical results based on the equation

$$P_{out} = \sigma_s(P_{in} - P_{th}), \quad (2)$$

where P_{out} is the output power, σ_s is the slope efficiency of the output versus the input, P_{in} is the incident pump power, and P_{th} is the threshold pump power.

The highest output power of 8.09 W was achieved at an incident pump power of 19.4 W with 11% transmission for the output coupler, thus resulting in an optical conversion efficiency of 41.7% and a slope efficiency of 54.6%. The results indicated that the laser performance of Nd:$Lu_{0.99}La_{0.01}VO_4$ reached[11–14,16] and even surpassed[10,15,17] those of other mixed laser crystals. When the output coupler was replaced by a mirror with transmissions of 7%, 20%, and 30%, the highest values of the obtained output power were 6.77, 7.72, and 7.09 W, respectively, at a pump power of 19.4 W. The output power values correspond to optical conversion efficiencies of 34.9%, 39.8%, and 36.6%. No saturation phenomenon appeared at the transmissions of 11%, 20%, and 30% in our experiment, thus indicating that higher output power can be achieved by increasing pump power. However, at the transmission of 7%, severe thermal effects caused the operating state to get near the edge of the stable region. Moreover, the output power exhibited some saturation phenomena.

Figure 5 shows the laser spectrum recorded by the optical spectrum analyzer. The central wavelength of the CW laser was 1065.97 nm, and the FWHM of the laser

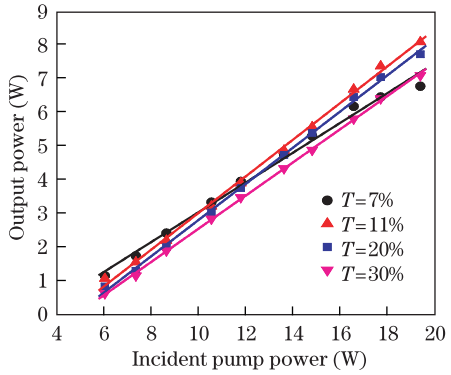

Fig. 4. Laser output power versus incident pump power.

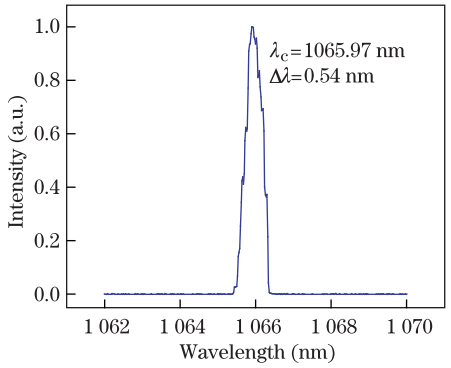

Fig. 5. Laser spectrum of Nd:$Lu_{0.99}La_{0.01}VO_4$.

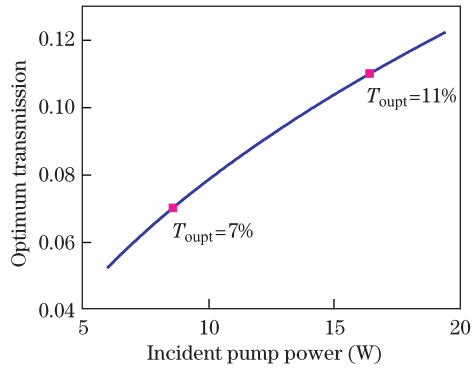

Fig. 6. Change in the optimum transmission of the output coupler with pump power.

spectrum was 0.54 nm. The difference between the peak emission wavelength of the fluorescence spectrum and that of the laser spectrum was caused by the balance among the transmittance curve of the mirrors, the gain curve of the laser crystal, and the resonant longitudinal modes.

Figure 4 also shows that when the pump power was lower than 11.8 W, the maximum output power was obtained at 7% transmission, whereas when the pump power varied from 11.8 to 19.4 W, the maximum output power was achieved at 11% transmission. According to Ref. [22], the optimum transmission of the output coupler $T_{\rm opt}$ can be calculated by

$$-\ln(1-T_{\rm opt}) = (\sqrt{2g_0 l/\delta} - 1)\delta, \quad (3)$$

$$g_0 = \frac{\eta}{I_{\rm s} A l} P_{\rm in}, \quad (4)$$

where δ is the intracavity loss, l is the length of the active material, g_0 is the small signal gain coefficient, η is the total pump efficiency, $I_{\rm s}$ is the saturable intensity, A is the effective area of the mode, and $P_{\rm in}$ is the pump power. By using the Findlay-Clay method, the intracavity loss δ of 0.0426, as well as the product of the small signal gain g_0 and the crystal length l of $0.018P_{\rm in}$, was determined. The optimum transmission of the output coupler versus the pump power was then solved through the numerical simulations of Eqs. (3) and (4). The results are shown in Fig. 6, which indicates that optimum transmission increased from 5.2% to 12.2% as pump power increased from 6 to 19.4 W. Furthermore, 7% transmission was considerably nearer the optimum value at low pump power, thus implying that higher output power can be obtained with this transmission. Meanwhile, 11% transmission gradually became closer to the optimum value as pump power increases, thus indicating that higher output power can be achieved with 11% than with 7% transmission. The theoretical analyses exhibit good agreement with the experimental results. An output coupler with 11% transmission or more is expected to obtain high output power at high pump power.

The TEM_{00} mode sizes at the laser crystal $w_{\rm g}$ and the output coupler $w_{\rm oc}$ were calculated by using ABCD matrix theory and the fitted thermal focal length, as shown in Eq. (1). The results were plotted as a function of the incident pump power in Fig. 3. When the pump power increased from 8 to 20 W, $w_{\rm g}$ became smaller than the pump beam width, thus resulting in the reduction of overlapping efficiency and the possibility of a multimode operation. Meanwhile, $w_{\rm oc}$ was also decreased with increasing pump power, which corresponds to an increase in the divergence angle of the laser beam. This finding is consistent with the experimental phenomenon. High output power and efficiency are expected to be achieved by optimizing the resonator design, such as by applying a plane-concave cavity to increase $w_{\rm g}$ and overlapping efficiency.

In conclusion, we report on the fluorescence spectrum of the novel mixed crystal Nd:$Lu_{0.99}La_{0.01}VO_4$. We also measure the thermal focal length of this new crystal. A diode end-pumped CW laser operation of Nd:$Lu_{0.99}La_{0.01}VO_4$ at 1065.97 nm is successfully demonstrated. The CW output characteristics are investigated by using different output couplers at 7%, 11%, 20%, and 30% transmissions. A maximum CW output power of 8.09 W is obtained at an incident pump power of 19.4 W, which corresponds to an optical-to-optical conversion efficiency of 41.7% and a slope efficiency of 54.6%. The experimental results show that Nd:$Lu_{0.99}La_{0.01}VO_4$ crystal may be a promising gain crystal for end-pumped solid-state lasers.

This work was supported by the Natural Science Foundation of Shandong Province (No. ZR2010FM029) and the Interdisciplinary Incubation Project Foundation of the Shandong University (No. 2011JC025).

References

1. A. Y. Yao, W. Hou, Y. P. Kong, L. Guo, L. A. Wu, R. N. Li, D. F. Cui, Z. Y. Xu, Y. Bi, and Y. Zhou, J. Opt. Soc. Am. B **22,** 2129 (2005).

2. H. B. Qin, Z. Zhuo, J. Liu, H. B. Zhang, and Y. G. Wang, Laser Phys. **21,** 1562 (2011).
3. F. Li, N. Zong, Z. Wang, L. Han, Y. Bo, Q. Peng, D. Cui, and Z. Xu, Chin. Opt. Lett. **9,** 041405 (2011).
4. H. Zhang, J. Liu, J. Wang, C. Wang, L. Zhu, Z. Shao, X. Meng, X. Hu, M. Jiang, and Y. T. Chow, J. Opt. Soc. Am. B **19,** 18 (2002).
5. J. Yang, J. Liu, and J. He, Laser Phys. Lett. **2,** 171 (2005).
6. V. Lupei, N. Pavel, Y. Sato, and T. Taira, Opt. Lett. **28,** 2366 (2003).
7. C. Maunier, J. L. Doualan, R. Moncorg, A. Speghini, M. Bettinelli, and E. Cavalli, J. Opt. Soc. Am. B **19,** 1794 (2002).
8. S. Zhao, H. Zhang, J. Liu, J. Wang, X. Xu, Z. Zhao, J. Xu, and M. Jiang, J. Crys. Growth **279,** 146 (2005).
9. H. Zhang, J. Liu, J. Wang, X. Xu, and M. Jiang, Appl. Opt. **44,** 7439 (2005).
10. V. G. Ostroumov, G. Huber, A. I. Zagumennyi, Y. D. Zavartsev, P. A. Studenikin, and I. A. Shcherbakov, Opt. Commun. **124,** 63 (1996).
11. Z. Zhuo, T. Li, S. G. Li, B. Zhao, J. Z. Chen, and S. S. Li, Laser Phys. Lett. **6,** 445 (2009).
12. H. H. Xu, H. H. Yu, Z. P. Wang, S. Han, Y. C. Wang, Z. B. Pan, Y. Y. Zhang, S. Q. Sun, J. Y. Wang, and H. J. Zhang, Opt. Express **20,** 16524 (2012).
13. Z. Zhuo, S. G. Li, T. Li, J. M. Jiang, C. X. Shan, J. Li, B. Zhao, and J. Z. Chen, Laser Phys. Lett. **7,** 116 (2010).
14. S. Zhang, L. Xu, M. Wang, H. Peng, F. Chen, J. Xu, and B. Zhao, Laser Phys. Lett. **7,** 339 (2010).
15. H. H. Yu, Y. G. Yu, H. J. Zhang, Z. P. Wang, J. Y. Wang, X. F. Cheng, Z. S. Shao, and M. H. Jiang, J. Crystal Growth **293,** 394 (2006).
16. Y. Yu, J. Wang, H. Zhang, H. Yu, Z. Wang, M. Jiang, H. Xia, and R. I. Boughton, J. Opt. Soc. Am. B **25,** 995 (2008).
17. S. Y. Zhang, H. T. Huang, M. J. Wang, L. Xu, W. B. Chen, J. Q. Xu, J. L. He, and B. Zhao, Laser Phys. Lett. **8,** 189 (2011).
18. G. Huang, B. Zhao, Y. Yu, C. Du, Y. Guo, S. Ruan, and J. Chen, Opt. Commun. **285,** 5375 (2012).
19. M. R. B. Andreeta, A. S. S. de Camargo, L. A. O. Nunes, and A. C. Hernandes, J. Crystal Growth **291,** 117 (2006).
20. J. H. Liu, J. R. Lu, J. H. Lu, Z. S. Shao, and M. H. Jiang, Chin. Phys. Lett. **16,** 181 (1999).
21. M. E. Innocenzi, H. T. Yura, C. L. Fincher, and R. A. Fields, Appl. Phys. Lett. **56,** 1831 (1990).
22. W. Koechner, *Solid-State Laser Engineering* (6th ed.) (Springer, New York, 2006).